Ocean Dynamics
https://doi.org/10.1007/s10236-017-1116-6

# Numerical modeling of general circulation, thermohaline structure, and residence time in Gorgan Bay, Iran

**Mohammad Hassan Ranjbar** [1] **· Nasser Hadjizadeh Zaker** [1]

Received: 22 September 2016 / Accepted: 26 October 2017
© Springer-Verlag GmbH Germany 2017

**Abstract** Gorgan Bay is a semi-enclosed basin located in the southeast of the Caspian Sea, Iran. The bay is recognized as a resting place for migratory birds as well as a spawning habitat for native fish. However, apparently, no detailed research on its physical processes has previously been conducted. In this study, a 3D coupled hydrodynamic and solute transport model was used to investigate general circulation, thermohaline structure, and residence time in Gorgan Bay. Model outputs were validated against a set of field observations. Bottom friction and attenuation coefficient of light intensity were tuned in order to achieve optimum agreement with the observations. Results revealed that, due to the interaction between bathymetry and prevailing winds, a barotropic double-gyre circulation, dominating the general circulation, existed during all seasons in Gorgan Bay. Furthermore, temperature and salinity fluctuations in the bay were seasonal, due to the seasonal variability of atmospheric fluxes. Results also indicated that under the prevailing winds, the domain-averaged residence time in Gorgan Bay would be approximately 95 days. The rivers discharging into Gorgan Bay are considered as the main sources of nutrients in the bay. Since their mouths are located in the area with a residence time of over 100 days, Gorgan Bay could be at risk of eutrophication; it is necessary to adopt preventive measures against water quality degradation.

**Keywords** Double gyre · Gorgan Bay · Inverse estuary · MIKE 3 Flow Model FM · Salinity and temperature

Responsible Editor: Sandro Carniel

✉ Mohammad Hassan Ranjbar
hassan.ranjbar@ut.ac.ir

[1] Graduate Faculty of Environment, University of Tehran, Tehran, Iran

## 1 Introduction

Gorgan Bay (36.77–36.92° N and 53.42–54.05° E) is a relatively shallow, semi-enclosed basin located at the southeastern section of the Caspian Sea in Iran, with a length of about 60 km, a maximum width of 12 km, an average depth of 1.8 m, and a maximum depth of 5 m in central portion of the bay (Fig. 1).

Covering an area of about 667 km$^2$, Gorgan Bay has an approximate volume of 1.2 km$^3$. The bay is bounded to the south by Alborz Mountain Range, to the east by Turkmen Sahra, to the west by Mazandaran Province, and to the north partially by the Caspian Sea and partially by Miankaleh Peninsula—an elongated barrier system which separates the bay from the Caspian Sea.

Gorgan Bay is connected with the Caspian Sea through an inlet (hereafter called primary inlet) with a width of about 3 km in the north-eastern corner of the bay. Khozini Channel, which is 6 km to the west of the primary inlet, is another connection between the bay and the Caspian Sea. The channel's width is about 200 m (Fig. 1). Therefore, the bay is relatively isolated from the sea and is characterized by significantly low wave energy (Bastami et al. 2012). The water level fluctuation due to tide is very negligible in the Caspian Sea and consequently in Gorgan Bay. Therefore, tidal impacts on physical processes can be ignored in comparison with the effects of wind and density gradients in Gorgan Bay (Kosarev 2005; Kitazawa and Yang 2012).

Considering data obtained from a synoptic weather station located next to the primary inlet of the bay, the annual prevailing wind in the study area is westerly with a mean speed of 5 m/s; however, it has seasonal fluctuations. Winds over Gorgan Bay are dominantly westerly and northwesterly from January to October, northeasterly and easterly in November, and again westerly and easterly in December.

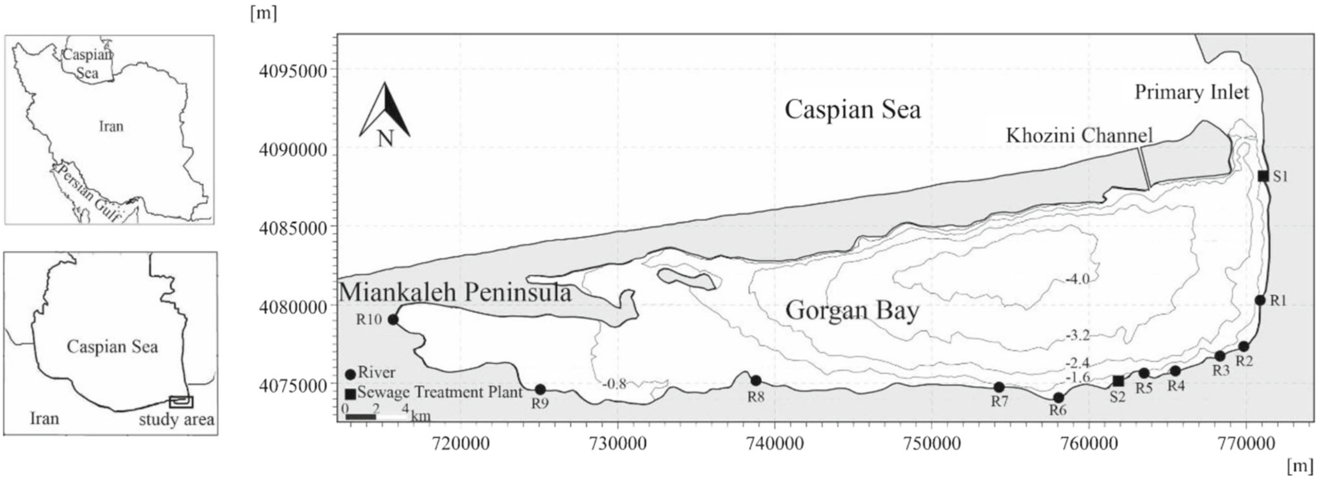


**Fig. 1** Gorgan Bay, Iran. Pollution sources are labeled. The circles and squares are rivers and sewage treatment plants, respectively. The water depth is in meters. The coordinate system refers to UTM-39 zone

The sum of all the fresh water entering Gorgan Bay, through river discharge and precipitation, is very low; discharge of all the ten rivers into the bay is about 1.3 $m^3$/s, and precipitation rate is 30.7 cm/year for the whole area under study. Nevertheless, evaporation is significantly stronger: it amounts to 124.1 cm/year. Therefore, the bay is an evaporation basin and behaves like an inverse estuary; hence, saltier, denser water is formed in the bay. The Caspian Sea provides water for deficiency through the inlets and, accordingly, the mean annual flow due to this water level tilting is about 26 $m^3$/s.

The rivers discharging into the bay, including Qareh Sou (R1), Kurdkuy (R2), Kar kandeh (R3), Baghu (R4), Gaz (R5), Now Kandeh (R6), Galugah (R7), Rostamkola (R8), Behshahr (R9), and Zagh Marz (R10), pass through agricultural lands and urban areas and transport aquatic plant nutrients and several pollutants into the bay (Bastami et al. 2012). Qareh Sou River, located in the southeast corner of the bay (Fig. 1), is the most important one, having the greatest water flow, with a flow of 800 L/s (Kurdi et al. 2015). Two cities, Bandar Torkaman and Bandar Gaz with populations of around 50,000 and 46,000 respectively, are located next to the bay. Polluted water from sewage treatment plants of these cities, hereafter called W1 and W2, pour into the bay, which is considered as another source of nutrients (Fig. 1).

Water quality and eutrophication in semi-enclosed coastal water bodies depend on their physical, chemical, and biological processes, which are mainly controlled by the rate of water exchange between the water body and its adjacent open sea (Yuan et al. 2007; Arega et al. 2008). Residence time is a concept relative to water exchange. Residence time can be defined as the time spent by a volume of water to leave a water body through its inlet (Luff and Pohlmann 1996; Wan et al. 2013).

This study used numerical modeling to address three main goals: (1) to depict wind-induced circulations in the bay, (2) to illustrate the general circulation and thermohaline structure in the study area, and (3) to calculate the residence time in Gorgan Bay. This study seems to be the first to investigate the detailed general circulation of Gorgan Bay, its thermohaline structure, and the residence time in the bay.

## 2 Material and methods

To determine general circulation, thermohaline structure, and residence time in Gorgan Bay, a 3D coupled hydrodynamic and solute transport numerical model was used. In addition, under different scenarios, the most influential parameter on hydrodynamics of the bay was determined and also residence time was estimated.

### 2.1 The numerical model

This study employed the MIKE 3 Flow Model FM. This model was developed by the Danish Hydraulic Institute (DHI) for three-dimensional water modeling. Being generally and scientifically acknowledged in the world, the MIKE 3 Flow Model FM is widely used by researchers (Payandeh et al. 2015; Fourniotis and Horsch 2015; Mahanty et al. 2016; Schoen et al. 2014). FM refers to the flexible mesh, on which the numerical techniques used in the modeling system are based (DHI 2012).

The MIKE 3 Flow Model FM is composed of several modules such as hydrodynamic module, ecological module, particle tracking module, transport module, mud transport module, and sand transport module (DHI 2012). In this study, the hydrodynamic and transport modules were used. Using a cell-centered finite volume method, the hydrodynamic module solves the 3D incompressible Reynolds-averaged Navier-Stokes equations, under the hydrostatic and Boussinesq assumptions. Local continuity equation (Eq. (1)) and horizontal momentum equations for $x$ and $y$ components (Eq. (2) and

(3)), governing equations of this module, are presented using Cartesian coordinates:

$$\frac{\partial u}{\partial x}+\frac{\partial v}{\partial y}+\frac{\partial w}{\partial z}=S \tag{1}$$

$$\begin{aligned}&\frac{\partial u}{\partial t}+\frac{\partial u^2}{\partial x}+\frac{\partial vu}{\partial y}+\frac{\partial wu}{\partial z}\\&=fv-g\frac{\partial \eta}{\partial x}-\frac{1}{\rho_0}\frac{\partial p_a}{\partial x}-\frac{g}{\rho_0}\int_z^\eta \frac{\partial \rho}{\partial x}dz-\frac{1}{\rho_0 h}\left(\frac{\partial s_{xx}}{\partial x}+\frac{\partial s_{xy}}{\partial y}\right)\\&+F_u+\frac{\partial}{\partial z}\left(v_t\frac{\partial u}{\partial z}\right)+u_sS\end{aligned} \tag{2}$$

$$\begin{aligned}&\frac{\partial v}{\partial t}+\frac{\partial v^2}{\partial y}+\frac{\partial uv}{\partial x}+\frac{\partial wv}{\partial z}\\&=-fu-g\frac{\partial \eta}{\partial y}-\frac{1}{\rho_0}\frac{\partial p_a}{\partial y}-\frac{g}{\rho_0}\int_z^\eta \frac{\partial \rho}{\partial y}dz-\frac{1}{\rho_0 h}\left(\frac{\partial s_{yx}}{\partial x}+\frac{\partial s_{yy}}{\partial y}\right)\\&+F_v+\frac{\partial}{\partial z}\left(v_t\frac{\partial v}{\partial z}\right)+v_sS\end{aligned} \tag{3}$$

where $t$ is the time; $x$, $y$, and $z$ are the Cartesian coordinates; $\eta$ is the surface elevation; $d$ is the still water depth; $h=\eta+d$ is the local water depth; $u$, $v$, and $w$ are the velocity components in $x$, $y$, and $z$ directions; $f=2\Omega\sin\Phi$ is the Coriolis parameter; $\Omega$ is the angular rate of revolution; $\phi$ is the geographic latitude; $g$ is the gravitational acceleration; $\rho$ is the density of water; $s_{xx}$, $s_{xy}$, $s_{yx}$, and $s_{yy}$ are components of the radiation stress tensor; $v_t$ is the vertical turbulent (or eddy) viscosity; $p_a$ is the atmospheric pressure; and $\rho_0$ is the reference density of water. Furthermore, $S$ is the discharge magnitude due to point sources and $(u_s, v_s)$ is the velocity by which the water is discharged into the ambient water (DHI 2012). The bottom stress in the hydrodynamic module, $\overrightarrow{\tau_b}=(\tau_{bx},\tau_{by})$, is determined by a quadratic friction law:

$$\frac{\overrightarrow{\tau_b}}{\rho_0}=c_f\overrightarrow{u}_b\left|\overrightarrow{u}_b\right| \tag{4}$$

where $\overrightarrow{u}_b$ is the velocity at a distance $\Delta z_b$ above the sea bed and the drag coefficient, $c_f$, is determined by assuming a logarithmic profile between the seabed and a point $\Delta z_b$ above the seabed:

$$c_f=\frac{1}{\left(\frac{1}{k}ln\left(\frac{\Delta z_b}{z_0}\right)\right)^2} \tag{5}$$

where $\kappa$=0.4 is the von Kármán constant and $z_0$ is the bed roughness length scale. When the boundary surface is rough, $z_0$ depends on the roughness height $k_s$:

$$z_0=mk_s \tag{6}$$

where $m$ is approximately 1/30 (DHI 2012).

The MIKE 3 Flow Model FM transport module, another module that was used in this study, is dynamically linked to the hydrodynamic module and simulates the spreading and fate of dissolved or suspended substances in a water environment under the influence of the fluid transport and associated dispersion processes. Today, there are numerous studies using this module (Cavalcante et al. 2012; Payandeh et al. 2015; Jiang et al. 2016). The transport module can calculate the transport of a scalar quantity. The conservation equation for a scalar quantity is given by the following:

$$\frac{\partial C}{\partial t}+\frac{\partial uC}{\partial x}+\frac{\partial vC}{\partial y}+\frac{\partial wC}{\partial z}=F_C+\frac{\partial}{\partial z}\left(D_v\frac{\partial C}{\partial z}\right)-k_PC+C_SS \tag{7}$$

where $D_v$ is vertical turbulent (eddy) diffusion coefficient, $C$ is concentration of scalar quantity, $k_P$ is linear decay rate of scalar quantity, $C_S$ is concentration of scalar quantity in source, and $F_C$ is horizontal diffusion term which is defined by the following:

$$F_C=\left[\frac{\partial}{\partial x}\left(D_h\frac{\partial}{\partial x}\right)+\frac{\partial}{\partial y}\left(D_h\frac{\partial}{\partial y}\right)\right]C \tag{8}$$

where $D_h$ is horizontal diffusion coefficient. Further information is available in the MIKE 3 Flow Model scientific documentation presented by DHI (DHI 2012).

### 2.2 Simulations setup

In this study, the MIKE mesh generator was used to produce a computational mesh. Mesh generation included the following steps: (1) selecting the area to be modeled by drawing boundaries; (2) defining the type of model boundaries and distinguishing open boundaries, through which water flows, from closed boundaries, through which water cannot pass; (3) generating depth independent triangular cells within the study area; (4) interpolating the bathymetry to the triangular cells; and (5) refining the cells' size by scaling the cell areas according to water depth at every element center point. Bathymetry data of Gorgan Bay, which showed water depth at each geographical position, was measured by the Iran National Cartographic Center in 2006 (data available at www.ncc.org.ir). The size of the cells varied spatially across the bay; in the shallower parts of the bay, the spatial grid resolution was made finer, and conversely. The resolution ranged from 300 m, on the coastline, to 500 m, in the deepest part of the bay. Generally, it can be said that the average area of the cells was around 47,700 m$^2$ (Fig. 2). In addition, the model had five vertical sigma layers.

Meteorological data, which were applied to the numerical model, were measured at a synoptic weather station belongs to Iran Meteorological Organization located just next to the primary inlet at 3-h intervals (data available at www.irimo.ir). Time series of the monthly discharges of the flowing rivers into the

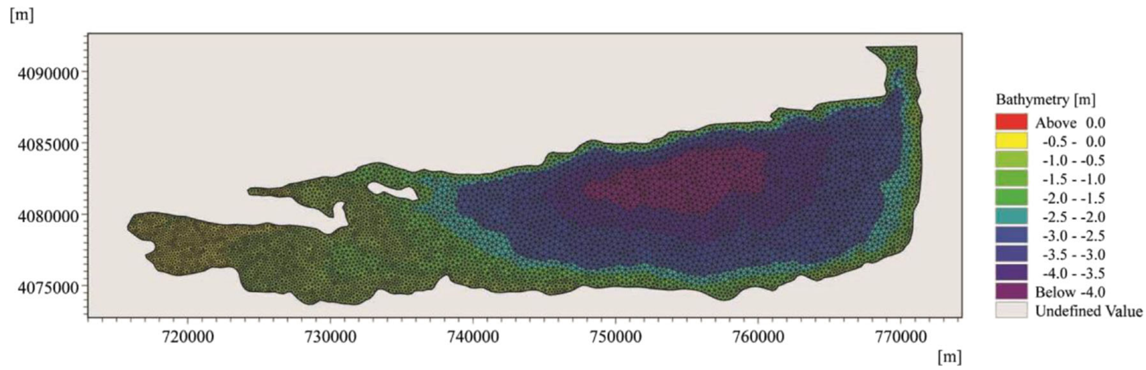


**Fig. 2** Bathymetric map and computational mesh for the model setup

bay, which were obtained from the hydrometric stations of the Iran Water Resources Management Company, were considered as point sources in the model (data available at www.wrm.ir).

The model which was used in this study had two types of boundaries: open boundaries, which include Gorgan Bay's primary inlet and Khozini Channel, and closed boundaries, namely its solid bottom and the coastlines. The water level was specified as the open boundary condition in the hydrodynamic model. Water level data at open boundaries was recorded by Iranian National Research Center of Caspian Sea, which is a branch of Iranian Water Research Institute, at a water level station with a time interval of 4 h (data available at www.wri.ac.ir). In addition, the water level of the bay was defined 27 m below the level of world oceans at the start of simulations.

This study consisted of five phases: (1) calibration, (2) validation, (3) modeling of wind-induced circulations, (4) modeling of general circulation and thermohaline structure, and (5) calculation of residence time. In phases 1 and 3, only effects of wind stress, bottom friction, and water level variations at the open boundaries were applied to the model. In other phases, modeling of Gorgan Bay was performed by considering water level changes, heat and salinity fluxes at the open boundaries, discharge impacts of the rivers, net precipitation, wind stress, bottom friction, and heat exchange with the atmosphere. The latter was calculated on the basis of latent heat flux, sensible heat flux, net shortwave radiation, and net longwave radiation. Therefore, heat and salt fluxes through open boundaries were also applied to the model, and time series of monthly variations of water temperature and salinity were used as other boundary conditions besides water level changes.

In tidal water bodies where rectilinear or reversing currents are predominant, it is typical that some tracers, released into a body of water, could leave the ambient during ebb period and return into their initial position during subsequent flood period. In this study, since there are almost no tides in the study area (Beni et al. 2013), it was assumed that no tracer leaving the bay through its open boundary, primary inlet, could ever return to the bay subsequently, and therefore, zero-tracer concentration was prescribed as the boundary condition in the transport model, in the fifth phase.

### 2.3 Field observation of surface currents

In order to provide data for calibration of numerical models, observations of surface currents in Gorgan Bay were made by surface drifters. The drifters had a cylindrical shape with a height of 1 m and cross diameter of 15 cm. The trajectories of the drifters were recorded by an internal Global Positioning System (GPS) device with a time interval of 1 min.

The floating drifters were launched in six different positions around the bay, as shown in Fig. 3. Each drifter deployed only one time at each site. Further information is presented in Table 1 to show how long each drifter was in operation and the length and the average speed of displacement of them.

## 3 Results and discussion

### 3.1 Sensitivity analysis and calibration

In order to yield reliable data, the numerical model needs to be calibrated. Calibration means the adjustment of modeling parameters to produce an adequate fit between the model outputs and the corresponding measurement data. In this study, the numerical model was calibrated against field observations of surface currents and a set of temperature and salinity measurement data.

Before calibration, the model's sensitivity to variations of the models parameters was investigated. The sensitivity analysis showed that the modeled current field was sensitive to grid cell size and bed roughness. The modeled temperature and salinity were also sensitive to grid cell size and attenuation of light intensity.

In order to make model outputs independent of grid cell size, the results obtained via different mesh resolutions were compared, the cell sizes were refined until steady results were achieved, and final mesh with optimum resolution was determined. All later simulations were carried out with the final mesh containing 12,882 horizontal cells (Fig. 2).

Considering the fact that currents in Gorgan Bay are mainly wind-driven currents, however, there was no more data

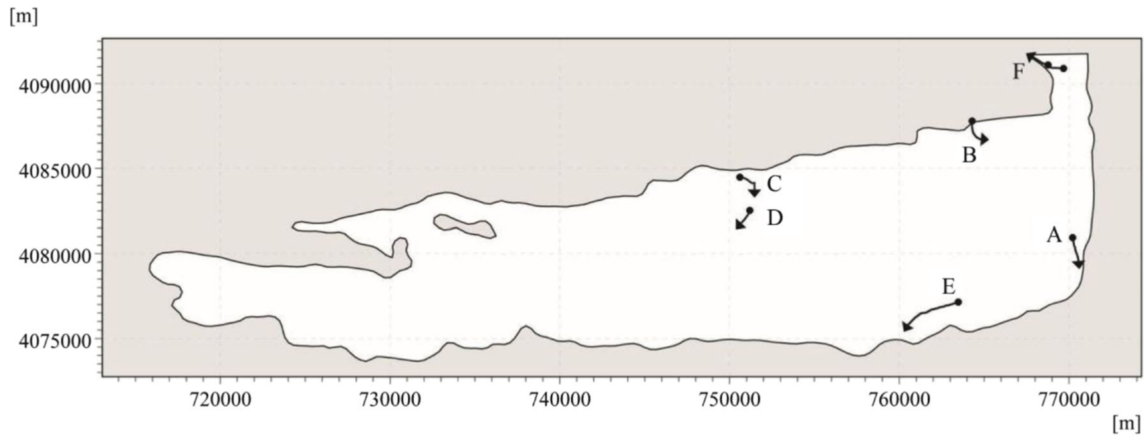


**Fig. 3** Schematic representation of the tracks of the drifter buoys

available; only wind forcing, bottom friction, and water level variations effects were considered for reproducing drifter trajectories. By comparing the field measurements of the Lagrangian trajectories of water mass with the corresponding model outputs and adjusting the value of the bottom friction to reduce any misfit, a total difference of 14.7% (total errors total length of displacements) was obtained between the modeled and measured trajectories (Fig. 4 and Table 2).

Since temperature and salinity affect physical processes in a water body, these parameters need to be calibrated as do currents in a hydrodynamic modeling. Bastami et al. (2014), using a CTD probe (Ocean Seven 316, Italy) that allows high resolution and simultaneous monitoring of pressure (expressed as water depth), temperature, pH, electrical conductivity (EC), dissolved oxygen concentration, total chlorophyll a concentration, turbidity, and light backscatter, measured temperature and salinity across Gorgan Bay in August 2010. In the present study, field data obtained from the mentioned study were used to calibrate the numerical model.

The modeled temperature and salinity were compared with the observed ones. By tuning the coefficient of attenuation of light intensity, differences between field measurements and model outputs were reduced. Table 3 shows the lowest obtained amount of difference between the modeled and the observed temperature and salinity in different points across the bay. Root mean square error (RMSE) method was used to quantify the differences between the modeled and observed data. A RMSE of 1.6 °C and 1.9 psu, pertaining to temperature and salinity, respectively, was obtained. Therefore, the simulation results, especially the temperature, were in good agreement with the observed data.

### 3.2 Wind-induced circulation in Gorgan Bay

Analysis of wind rose, created based on wind data measured in situ during year 2010, shows that winds mostly came from the west (25%) and the northwest (21%), while there was no wind during 21% of time and wind below with a speed of lower than 2 m/s over 4% of the time. Other directions have a frequency of 29%. Therefore, analysis shows prevailing wind below from the west sector. In addition, the average speed of prevailing wind was 5 m/s (Fig. 5).

In order to illustrate the effects of wind stress on general circulation in Gorgan Bay, currents induced by the prevailing wind, which is the westerly wind with a uniform speed of 5 m/s, were simulated using the hydrodynamic model. In this case, after a period of 2 days of simulation, the currents became stationary; therefore, the results that obtained from the third day are discussed below.

**Table 1** Details of the drifter program

| Drifter | Date of launching | Hour of launching | Location of deployment | | Operation time (min) | Displacement (m) | Average velocity (m/s) |
|---|---|---|---|---|---|---|---|
| A | 11/7/2013 | 7:00 | N 4080751 | E 235429.1 | 330 | 1296 | 0.065 |
| B | 11/7/2013 | 13:30 | N 4087578 | E 764287.0 | 400 | 1109 | 0.046 |
| C | 11/9/2013 | 7:00 | N 4084417 | E 750774.9 | 485 | 1058 | 0.036 |
| D | 11/9/2013 | 15:30 | N 4082344 | E 751124.4 | 225 | 743 | 0.055 |
| E | 11/10/2013 | 7:00 | N 4077051 | E 763285.3 | 960 | 2790 | 0.048 |
| F | 11/12/2013 | 7:00 | N 4090907 | E 234660.3 | 485 | 1671 | 0.057 |

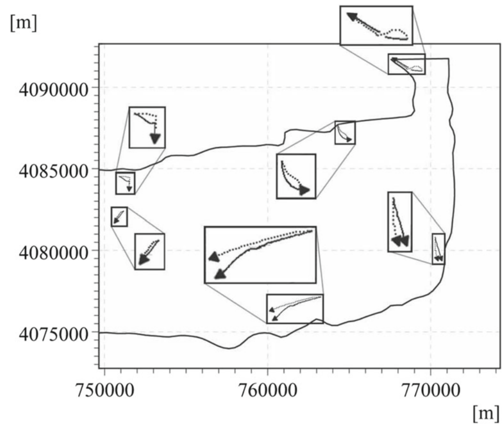


**Fig. 4** Observed and simulated (dotted line) drift trajectory data of the Lagrangian drifters

The results showed that surface currents were in the same direction as the wind in shallower areas and flowed in an opposite direction to the wind with a very slower speed where the bay is deeper, which is the central region of the bay. These currents caused a double-gyre circulation pattern: a cyclonic gyre in the southern part of the bay and a smaller anticyclonic gyre in the northern part (Fig. 6).

Furthermore, the current circulation pattern in the bottom layer was similar to that of the surface layer, but windward currents are weaker, and leeward ones are more severe in the bottom layer (Fig. 7). In this condition, the water levels across the entire bay increased monotonically in the same direction as the wind; surface elevation increased in the eastern part of the bay and decreased in the western part (Fig. 6).

An examination of the results of the studies by Csanady (1973) and Rueda and Vidal (2009) indicates that the interaction between varying topography and a steady wind stress can create horizontal changes in the currents. In this case, three major forces apply to a body of water: wind forcing, bed friction, and forces created by horizontal gradients of pressure, due to the slope of the sea surface. The two last forces are in an opposite direction to the wind. In shallower waters, the dominant force is wind stress, which causes a windward current, while dominant forces in deeper waters include bed friction and horizontal gradients of pressure, which cause a leeward current. This type of circulation pattern is called topographical gyres.

Figure 8 presents the vertical structure of the wind-induced currents in the central part (section A-A') of the bay due to a westerly wind with a speed of 5 m/s. The shallow margins of the bay, along the northern and southern coast, with a minimum depth, had the maximum current velocity in the same direction as the wind. With an increase in depth, velocity of windward currents decreased up to deeper areas where the return flow dominated. Afterwards, the velocity of leeward currents increased with an increase in depth (Fig. 7).

In addition, real wind-induced currents were modeled using time series of real wind conditions occurring between 2009 and 2010. Figures 9 and 10 show mean annual wind-induced circulation in Gorgan Bay. By comparison between Figs. 6 and 9, and besides, Figs. 7 and 10, it can be concluded that real wind-induced currents are deeply similar to currents induced by the prevailing wind, albeit weaker.

### 3.3 General circulation and thermohaline structure in Gorgan Bay

The general circulation and thermohaline structure induced by heat and salt fluxes through open boundaries, water surface and rivers, wind stress, river discharges, and water level fluctuation in Gorgan Bay were modeled using the hydrodynamic model. Adjustments from the initial conditions to actual conditions took almost 3 months for the temperature and nearly 4 months in the case of salinity. However, the results about the first year were ignored and only the results related to the second year of simulation were considered, as will be discussed in the following sections.

#### *3.3.1 General circulation in the bay*

Figures 11 and 12 show modeled mean annual general circulation of Gorgan Bay waters in both surface and bottom layers, respectively. Given the annual general circulation pattern in the bay and comparing it with wind-induced currents, it became evident that general circulation was a function of the wind-induced currents, in all

**Table 2** Accuracy of simulating of observed trajectories

| Drifter | Last observed point | | Last simulated point | | Error in easting (m) | Error in northing (m) | Total error (m) | Percent of error |
|---|---|---|---|---|---|---|---|---|
| A | N 4079668 | E 235632.2 | N 4079668 | E 235399.2 | 233 | 0 | 233 | 18 |
| B | N 4086821 | E 764894.0 | N 4087007 | E 764847.1 | 46.9 | 186 | 191.8 | 17.3 |
| C | N 4083903 | E 751523.1 | N 4084089 | E 751569.5 | 46.4 | 186 | 191.7 | 18.1 |
| D | N 4081927 | E 750803.4 | N 4081996 | E 750756.7 | 46.7 | 69 | 83.3 | 11.2 |
| E | N 4075940 | E 760551.2 | N 4076405 | E 760387.5 | 163.7 | 465 | 493 | 17.7 |
| F | N 4091658 | E 232890.1 | N 4091588 | E 232960.1 | 70 | 70 | 99 | 5.9 |

**Table 3** Comparison of simulated temperature and salinity versus observed data

| Station | Location | | Observed temperature | Modeled temperature | Observed salinity | Modeled salinity |
|---|---|---|---|---|---|---|
| 1 | N 36.92678 | E 54.02814 | 23.96 | 22.48 | 11.96 | 12.28 |
| 2 | N 36.90136 | E 54.03072 | 24.74 | 24.06 | 11.02 | 12.51 |
| 3 | N 36.85419 | E 54.03125 | 25.42 | 27.05 | 10.8 | 13.2 |
| 4 | N 36.81467 | E 54.03192 | 25.91 | 26.95 | 10.88 | 13.38 |
| 5 | N 36.87553 | E 53.90889 | 26.74 | 26.99 | 11.38 | 13.17 |
| 6 | N 36.83781 | E 53.90906 | 27.49 | 28.3 | 11.67 | 13.82 |
| 7 | N36.86936 | E 53.78997 | 25.22 | 27.86 | 11.36 | 13.41 |
| 8 | N 36.83289 | E 53.79058 | 26.2 | 28.12 | 11.33 | 13.66 |
| 9 | N 36.89981 | E 53.95894 | 26.55 | 23.78 | 11.31 | 12.67 |
| 10 | N 36.85264 | E 53.57528 | 25.54 | 26.76 | 12.4 | 13.83 |
| 11 | N 36.82233 | E 53.61694 | 26.91 | 27.08 | 11.67 | 13.75 |

the layers. In shallower areas, the transportation of water masses was eastward. In deeper areas, there was a westward transportation. Therefore, the circulation of water in Gorgan Bay was composed of two gyres: an anticyclonic one in the north and an intensified cyclonic one in the south. Like wind-induced currents, in the bottom layer, eastward currents became weaker and westward currents became stronger (Figs. 11 and 12). According to the seasonal fluctuation of currents, it was concluded that currents induced by prevailing winds are dominant throughout the year.

Based on the results, it was also revealed that mean annual velocity of currents in the whole bay is 5 cm/s, and Khozini Channel, having a small cross-sectional area, had the maximum current velocity of around 35 cm/s. In the primary inlet and shallow margins of the bay, current velocities were relatively high in comparison with other parts of the bay.

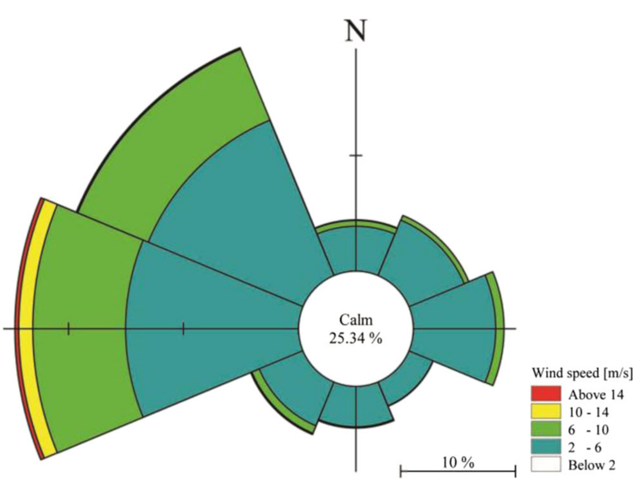


**Fig. 5** The wind rose of the study area in the study period

### *3.3.2 Thermohaline structures in the bay*

The results showed that domain-averaged temperature (DAT) and salinity fluctuated seasonally, caused by the seasonal variability of atmospheric fluxes. DAT directly followed the fluctuations of air temperature. However, domain-averaged salinity (DAS) followed the evaporation rate fluctuations, with a time lag of 2–3 months. DAT, air temperature, and evaporation rate reached their maximum values in July. On the other hand, DAS climbed to its maximum value in early October. DAT ranged from 5 to 29.2 °C, with the minimum occurring in late December, and DAS ranged from 12.3 to 15.2 psu, with the minimum being observed in February (Figs. 13 and 14).

The results showed that the mean annual water salinity increased monotonically in the northeast-southwest direction across the entire bay. In other words, salinity increased by distancing from the primary inlet (Fig. 11).

The fresh inflow of Caspian Sea water (ICSW) reduced the salinity in the northeast portion of the bay; during summer, ICSW affected a larger area in comparison with in winter, when it had a minimum effect. Most salty water masses ($S > 17$ psu) in Gorgan Bay were formed in the southwestern semi-enclosed basin where ICSW had the least effect on it (Fig. 11). It could be concluded that Gorgan Bay, like inverse estuaries, makes incoming water from the Caspian Sea saltier and denser.

Having the highest average inflow discharge, rivers located in the southeast corner of the bay, including Qareh Sou, Kurdkuy, and Kar kandeh, had a local effect on the bay's salinity. They reduced the salinity in the southeastern corner of the bay (Fig. 11).

Based on the model's results, the spatial variation of temperature of waters of Gorgan Bay was affected by topography and the distance from the primary inlet. Because of infiltration of colder water from the Caspian Sea, the regions located close to the open boundaries were always

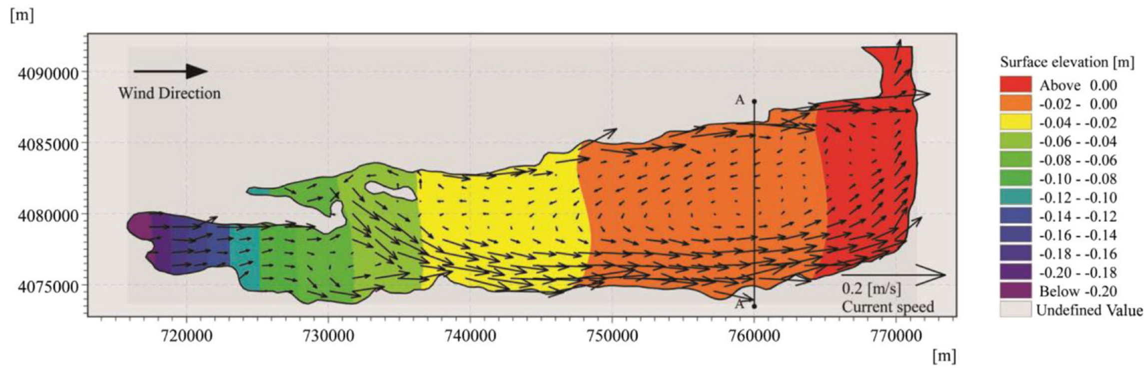


**Fig. 6** Wind-induced circulation in surface layer and water levels in Gorgan Bay under a westerly wind with a speed of 5 m/s

colder in comparison with other portions of the bay. In warm seasons, water temperature in Gorgan Bay had a linear east-west gradient; the western part was warmer than the eastern part, although the difference was a fraction of degree centigrade. During cold seasons, waters in the western, shallower part was colder than by around 1.5 °C in compassion with the central, deeper part (Fig. 12). During all of the seasons, Gorgan Bay showed a mixed layer behavior, and there was no stratification in the bay.

### 3.4 Residence time in Gorgan Bay

After the hydrodynamic model was calibrated, the hydrodynamic basis for coupling with other models was prepared and

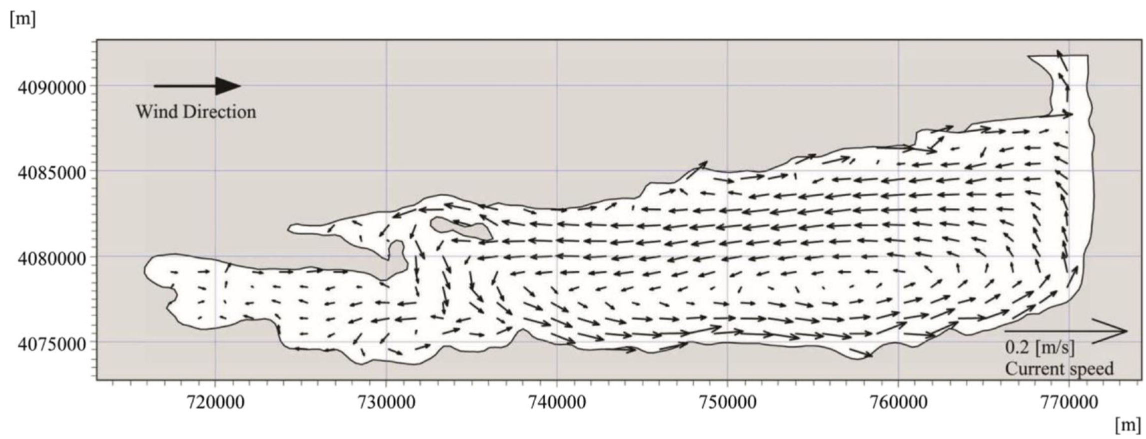


**Fig. 7** Wind-induced circulation in bottom layer in Gorgan Bay under a westerly wind with speed of 5 m/s

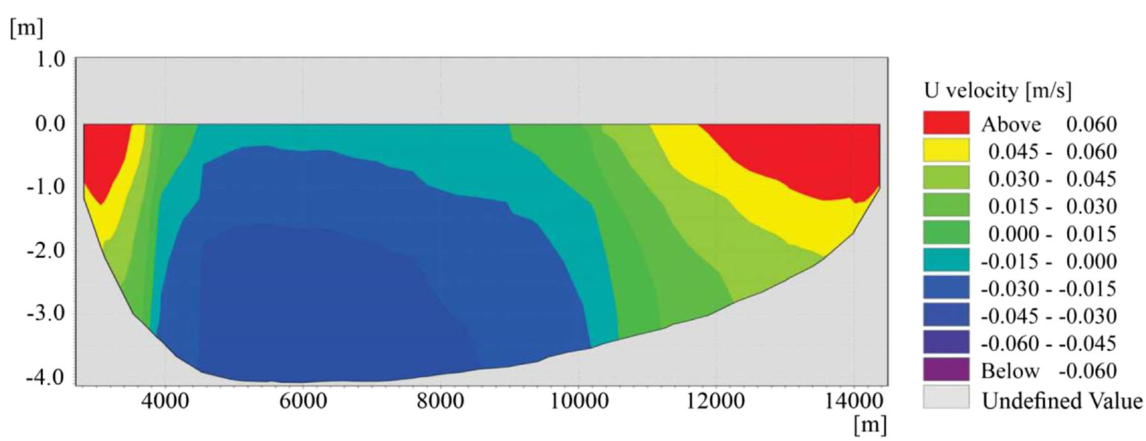


**Fig. 8** Cross section of velocity component in the *x* direction after 2 days of simulation due to a westerly wind with a speed of 5 m/s. Positive velocities point eastward. Section locations are shown in Fig. 5

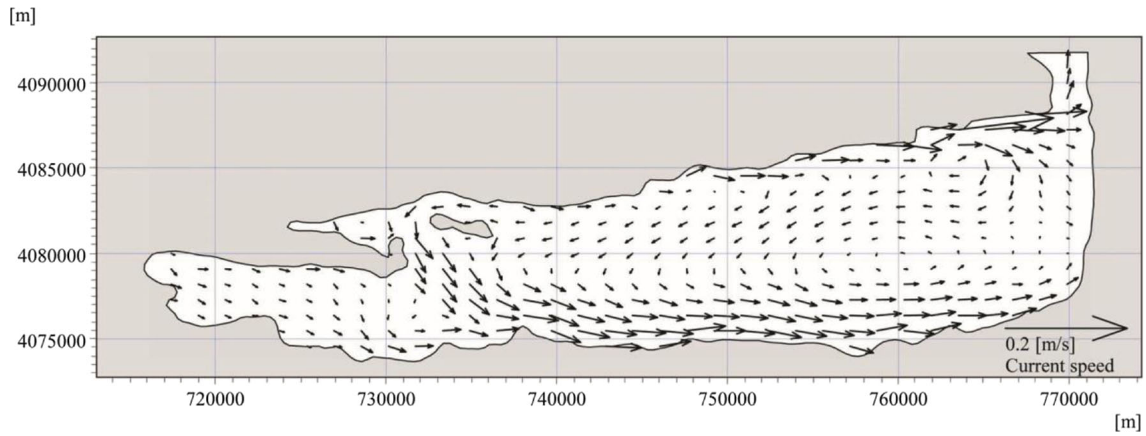


**Fig. 9** Mean annual wind-induced circulation in surface layer of Gorgan Bay

the transport model was coupled with the hydrodynamic model to estimate the residence time in the bay. Statistically, residence time has been shown to be equal to the time needed for a dissolved matter to fall to $1/e$ (~ 37%) of its initial concentration (Monsen et al. 2002; Thomann and Mueller 1987). This definition is widely used for the computation of residence time (Abdelrhman 2005; Cucco and Umgiesser 2006; Cavalcante et al. 2012; Wan et al. 2013). Therefore, initially, a unit concentration of passive dissolved conservative matter (PDCM) was placed in the bay and its dilution was then simulated with the coupled model. Simulation ended when constituents fell to 37% of their initial concentration in all parts of the bay.

Given the fact that residence time in a body of water varies with changes in external driving forces, simulations to

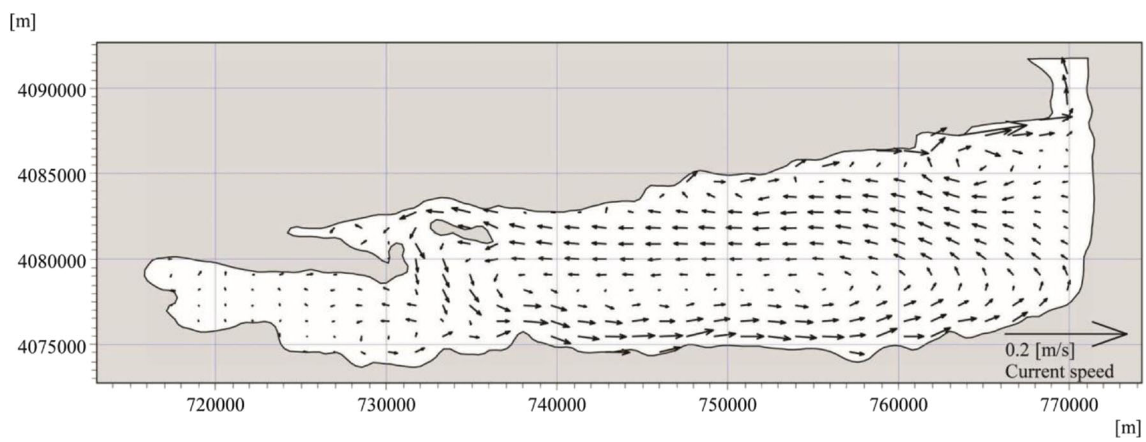


**Fig. 10** Mean annual wind-induced circulation in bottom layer of Gorgan Bay

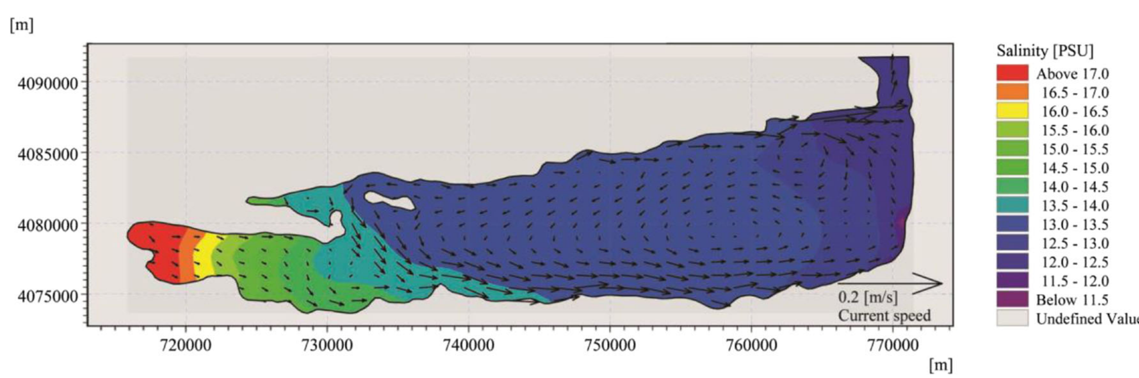


**Fig. 11** Mean annual general circulation pattern and the horizontal distributions of mean annual salinity in surface layer in Gorgan Bay

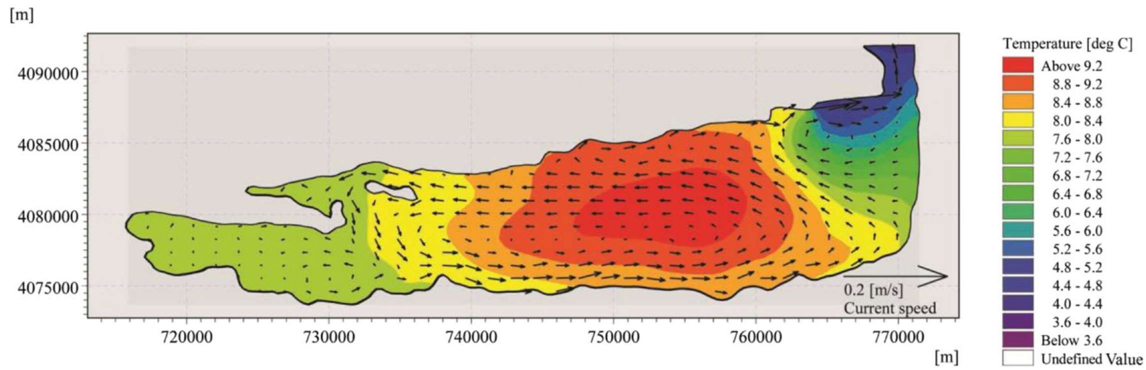


**Fig. 12** Mean annual general circulation pattern in bottom layer and the surface horizontal distributions of mean January temperature in Gorgan Bay

calculate the residence time were carried out under an idealized wind scenario, which was the wind blowing constantly eastward with a speed of 5 m/s.

The results showed that the domain-averaged residence time in Gorgan Bay was about 95 days. Because of the rapid mixing between bay waters and incoming waters form the Caspian Sea in the regions located close to the open boundaries, these areas of the bay had the shortest residence time and therefore, pollutants left this area over a shorter time. It is expectable that water quality problems within these areas will

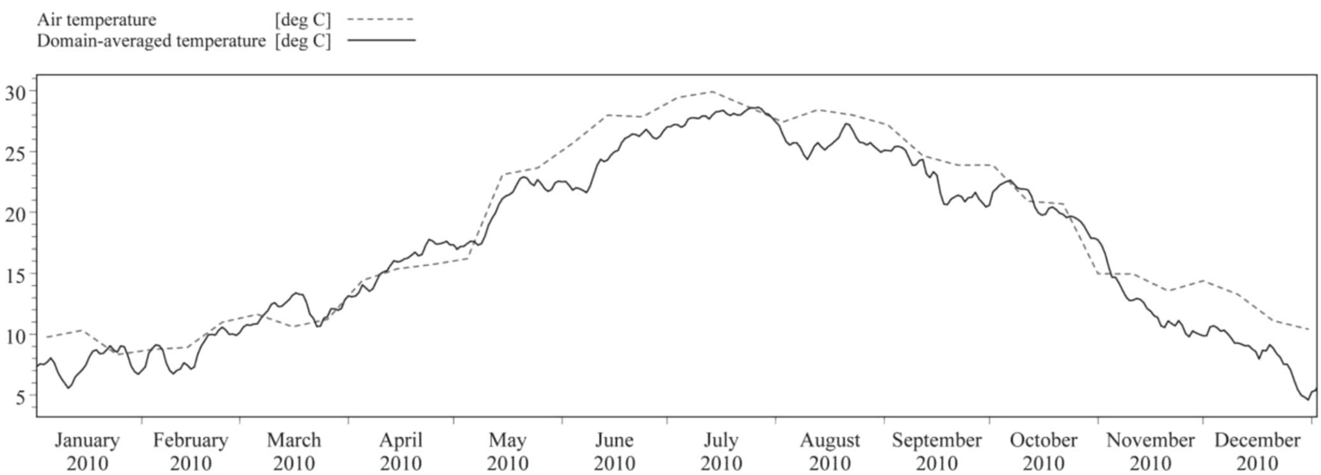


**Fig. 13** Time series of modeled domain-averaged water temperature and air temperature in Gorgan Bay, 2010

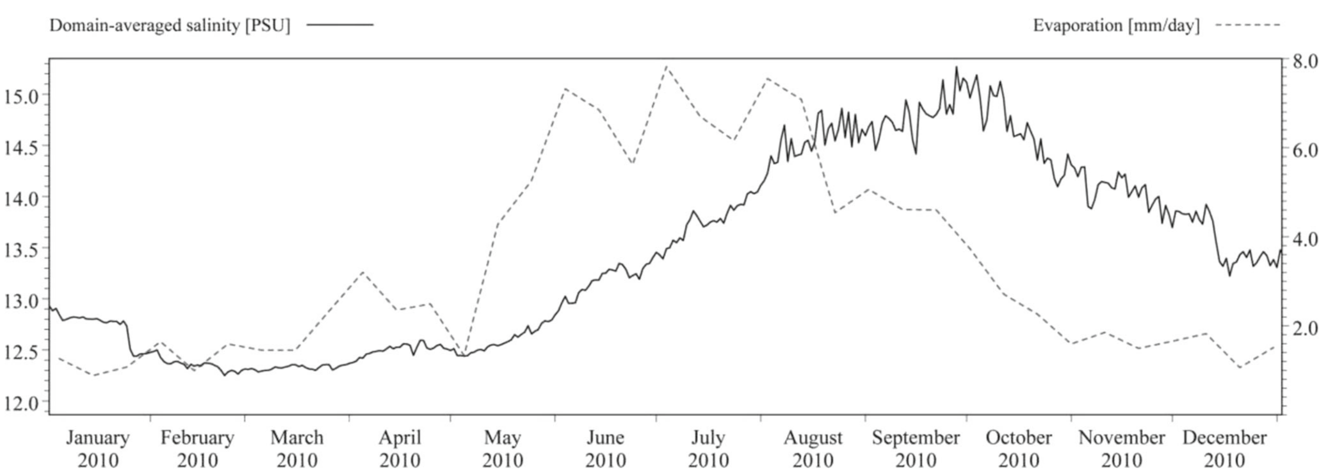


**Fig. 14** Time series of modeled domain-averaged water salinity and evaporation in Gorgan Bay, 2010

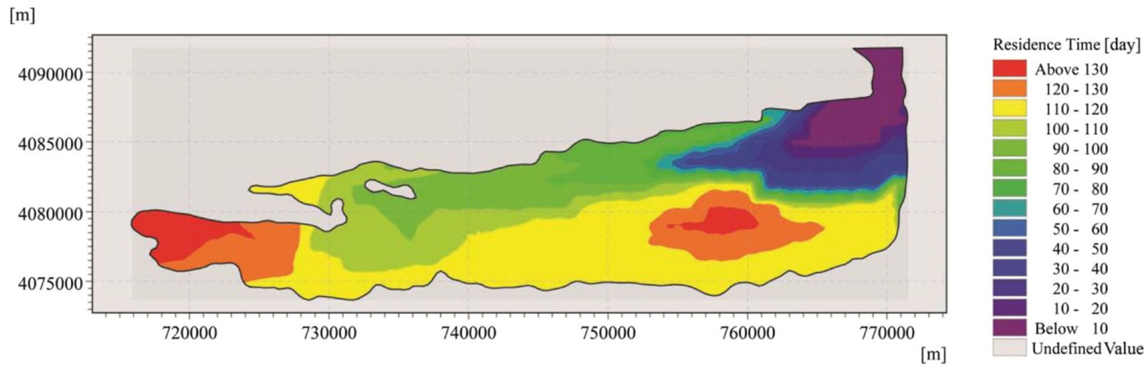


**Fig. 15** Spatial distribution of the residence time of the PDCM in Gorgan Bay

occur on scarce occasions (Brooks et al. 1999; Monsen et al. 2002; Cavalcante et al. 2012) (Fig. 15).

Topographical gyres caused PDCM to be trapped in the bottom half of the central portion of the bay where a relatively high residence time existed. The results showed that the semi-enclosed basin in the southwest corner of the bay, with the weakest diffusion capability in the study area, was isolated from other portions, and pollutants released in this region had less ability to leave the water body. Therefore, discharge from the pollution sources located in this area must be controlled (Fig. 15).

The southern region of the bay had a residence time of more than 100 days. Since all the rivers discharging into Gorgan Bay pass through agricultural and urban areas, they carry marine plant nutrients and their mouths are located in this region; adverse changes are forecasted in the trophic state of the bay. In order to prevent eutrophication, restriction of nutrient pollution sources along the rivers or taking appropriate measures to increase the mixing between Gorgan Bay and the Caspian Sea seems to be necessary.

In addition, residence time was estimated under four scenarios: (1) westerly wind blowing with a strength of 2.5 m/s, (2) westerly wind blowing with a strength of 5 m/s, (3) westerly wind blowing with a strength of 7.5 m/s, and (4) westerly wind blowing with a strength of 10 m/s. It was found that the residence time decreased with increase in the speed of wind blowing over the study area (Fig. 16).

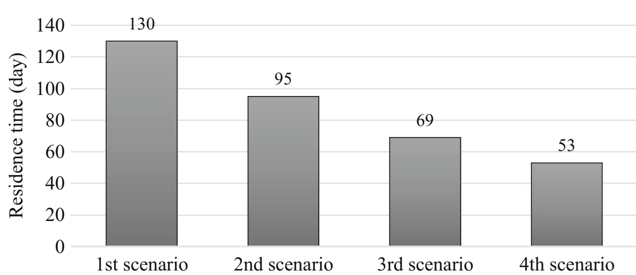


**Fig. 16** Comparing the residence time in Gorgan Bay under different scenarios

## 4 Conclusions

This study aimed at depicting general circulation, thermohaline structure, and residence time in Gorgan Bay. To this end, a numerical modeling study was carried out, and model outputs were validated against short-term field observations of surface currents and also a set of temperature and salinity measurement data. Firstly, a hydrodynamic model was used to study the wind-driven circulation of the bay under an idealized wind scenario. The results showed that the interaction between Gorgan Bay's topography and a steady wind stress could compose a double-gyre circulation in which along the shallow margins of the bay, currents were windward with relatively high velocity while in deeper currents the velocity was lower and in the opposite direction. Besides, it was also revealed that vertical variation was negligible.

Second, the hydrodynamic model was forced by considering heat and salt fluxes through open boundaries, water surface and rivers, wind stress, river discharges, and water level fluctuation to illustrate the general circulation and thermohaline structure in Gorgan Bay. Based on the results, it was revealed that general circulation was very similar to wind-driven circulation induced by prevailing winds in all seasons. Therefore, it could be concluded that topography and prevailing winds are two influential parameters in the formation of general circulation in Gorgan Bay. Results also showed salinity and temperature varied seasonally; in hot seasons, they reached their highest value and in cold seasons, they dropped to their minimum.

Finally, a transport model coupled with the calibrated hydrodynamic model was used to estimate residence time in Gorgan Bay. Results revealed that domain-averaged residence time in Gorgan Bay was about 95 days. Residence time in the bay varied spatially in such a way that a high potential for eutrophication could be expected.

**Acknowledgments** This study is part of the Master Thesis of the first author, which was supported by the Ports and Maritime Organization of Iran. The authors gratefully acknowledge this assistance.

## References


Abdelrhman MA (2005) Simplified modeling of flushing and residence times in 42 embayments in New England, USA, with special attention to Greenwich Bay, Rhode Island. Estuar Coast Shelf Sci 62: 339–351

Arega F, Armstrong S, Badr A (2008) Modeling of residence time in the East Scott Creek Estuary, South Carolina, USA. J Hydro Environ Res 2:99–108

Bastami K, Bagheri H, Haghparast S, Soltani F, Hamzehpoor A, Bastami M (2012) Geochemical and geo-statistical assessment of selected heavy metals in the surface sediments of Gorgan Bay, Iran. Mar Pollut Bull 64:2877–2884

Bastami KD, Taheri M, Bagheri H, Foshtomi MY, Ganji S, Haghparast S, Soltani F, Hamzehpoor A, Karimi B (2014) Response of sediment-dwelling annelida community in relation to geochemical parameters in the Gorgan bay, Caspian Sea. Int J Environ Sci Technol 11:2025–2036

Beni A, Lahijani H, Harami R, Arpe K, Leroy S, Marriner N, Berberian M, Andrieu-Ponel V, Djamali M, Mahboubi A, Reimer P (2013) Caspian sea-level changes during the last millennium: historical and geological evidence from the south Caspian Sea. Clim Past 9: 1645–1665

Brooks D, Baca M, Lo Y (1999) Tidal circulation and residence time in a macrotidal estuary: Cobscook Bay, Maine. Estuar Coast Shelf Sci 49:647–665

Cavalcante GH, Kjerfve B, Feary DA (2012) Examination of residence time and its relevance to water quality within a coastal mega-structure: the Palm Jumeirah Lagoon. J Hydrol 468:111–119

Csanady GT (1973) Wind-induced barotropic motions in long lakes. J Phys Oceanogr 3:429–438

Cucco A, Umgiesser G (2006) Modeling the Venice Lagoon residence time. Ecol Model 193:34–51

DHI (2012) MIKE 3 Flow Model user guide and scientific documentation

Fourniotis NT, Horsch GM (2015) Baroclinic circulation in the gulf of Patras (Greece). Ocean Eng 104:238–248

Jiang T, Zhong M, Cao Y, Zou L, Lin B, Zhu A (2016) Simulation of water quality under different reservoir regulation scenarios in the Tidal River. Water Resour Manag 30:3593–3607

Kitazawa D, Yang J (2012) Numerical analysis of water circulation and thermohaline structures in the Caspian Sea. J Mar Sci Technol 17: 168–180

Kosarev A (2005) Physico-geographical conditions of the Caspian Sea. In: The handbook of environmental chemistry. Springer

Kurdi M, Eslamkish T, Seyedali M, Ferdows M (2015) Water quality evaluation and trend analysis in the Qareh Sou Basin, Iran. Environ Earth Sci 73:8167–8175

Luff R, Pohlmann T (1996) Calculation of water exchange times in the ICES-boxes with a eulerian dispersion model using a half-life time approach. German J Hydrogr 47:287–299

Mahanty M, Mohanty P, Pattnaik A, Panda U, Pradhan S, Samal R (2016) Hydrodynamics, temperature/salinity variability and residence time in the Chilika lagoon during dry and wet period: measurement and modeling. Cont Shelf Res 125:28–43

Monsen N, Cloern J, Lucas L, Monismith S (2002) A comment on the use of flushing time, residence time and age as transport time scales. Limnol Oceanogr 47:1545–1553

Payandeh A, Hadjizadeh Zaker N, Niksokhan M (2015) Numerical modeling of pollutant load accumulation in the Musa estuary, Persian Gulf. Environ Earth Sci 73:185–196

Rueda FJ, Vidal J (2009) Currents in the upper mixed layer and in unstratified water bodies. Encyclopedia of Inland Waters. Elsevier 568–582

Schoen JH, Stretch DD, Tirok K (2014) Wind-driven circulation patterns in a shallow estuarine lake: St Lucia, South Africa. Estuar Coast Shelf Sci 146:49–59

Thomann RV, Mueller JA (1987) Principles of surface water: quality modeling and control. HarperCollins, New York City

Wan Y, Qui C, Doering P, Ashton M, Sun D, Coley T (2013) Modeling residence time with a three-dimensional hydrodynamic model: linkage with chlorophyll a in a subtropical estuary. Ecol Model 268:93–102

Yuan D, Lin B, Falconer R (2007) A modelling study of residence time in a macro-tidal estuary. Estuar Coast Shelf Sci 71:401–411